Self-Assembly of Small Peptidomimetic Cyclophanes

Jorge Becerril,[a] M. Isabel Burguete,[a] Beatriu Escuder,*[a] Francisco Galindo,[a] Raquel Gavara,[a] Juan F. Miravet,[a] Santiago V. Luis,*[a] and Gabriel Peris[b]

Abstract: The self-assembly of a series of small peptidomimetic cyclophanes in organic solvents was studied. X-ray diffraction, NMR spectroscopy, and molecular modelling were used to understand the structural features of these self-assembling compounds both at the molecular and supramolecular level. The factors that could influence the formation of gels rather than crystals were studied and a model for the arrangement of molecules in the gel was proposed. Furthermore, scanning electron microscopy revealed that in some cases these compounds undergo a transcription of chirality when going from organogelator to helicoidal gel fibres.

Keywords: gels · helical structures · peptidomimetics · self-assembly · supramolecular chemistry

Introduction

In the last decade a large number of low molecular weight compounds capable of reversibly forming gels in both organic liquids and water have been reported.[1,2] This class of compounds is able to self-assemble into fibres of several micrometer length that further crosslink and entrap solvent molecules, thus affording a soft, solid-like material. The singular physical and chemical properties of these materials have resulted in studies focussing towards their development as novel functional materials for use in drug delivery processes, responsive materials, catalysis, and so forth.[3] The synthesis of chiral nano- and microstructures is of great interest in many fields of chemistry and technology. For example, organogels have been used as templates for the preparation of nanotubular materials such as the hollow helicoidal silicas prepared by Shinkai et al. in which a clear transcription of chirality from the molecular to the supramolecular level was observed. This is not always straightforward and generally requires precise design of a molecule with appropriate functionalities.[4]

Unfortunately, in most cases the gelation ability of such compounds has been discovered serendipitously, and the results of the structural factors involved in the process seem to be quite dependent on the studied case. Nowadays, a major effort is directed towards the controlled design of compounds with the appropriate functionalities to obtain the desired gel. As a result, there is an intriguing question with regard to the transcription of information from the molecular level to the microscale supramolecular structure of these materials. Thus, although there are many techniques such as electron microscopy and X-ray and neutron scattering techniques (SAXS, SANS, etc.) to study the microscopic features of the gels, it remains difficult to obtain direct information about the individual molecular organisation inside the fibres. One of the most convenient approaches to undertake this objective is to obtain indirect structural information through the study of structurally related compounds that have single crystal structures available.[5]

Among the diverse number of low molecular weight structures found to form gels in organic solvents, amino acid fragments are one of the most common building blocks.[6] For instance, some time ago the Z-protected acyclic precursors of **1**–**5** were reported as good organogelators, their gelation ability being based on the presence of the carbamate group (Scheme 1).[7] Other examples of low molecular weight organogelators that contain peptides are found in the literature, but only a few of these are cyclic peptidomimetic organogelators.[8] Recently, we found that peptidomimetic cyclophanes that contain L-valine such as **8b** and **8c** were able to form gels in organic solvents.[9] Here we report on the synthesis and study of those molecules as well as several closely related analogues. The main aim of this work is to highlight the structural features responsible for their assembly.

[a] J. Becerril, Dr. M. I. Burguete, Dr. B. Escuder, Dr. F. Galindo, R. Gavara, Dr. J. F. Miravet, Prof. Dr. S. V. Luis
Departament de Química Inorgànica i Orgànica
Universitat Jaume I, 12071 Castelló (Spain)
Fax: (+34) 964-728-214
E-mail: escuder@qio.uji.es

[b] Dr. G. Peris
Serveis Centrals d'Instrumentació Científica
Universitat Jaume I, 12071 Castelló (Spain)

Supporting information for this article is available on the WWW under http://www.chemeurj.org/ or from the author.

 DOI: 10.1002/chem.200400031

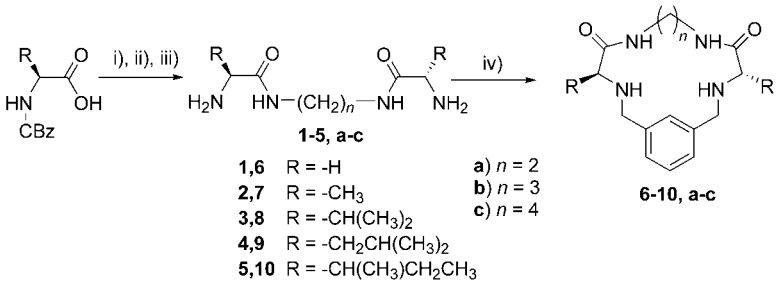

Scheme 1. i) *N*-hydroxysuccinimide, DCC, THF, 0 °C; ii) $H_2N(CH_2)_nNH_2$, DME, room temperature; iii) HBr in AcOH (33 %, basic work-up; and iv) 1,3-bis(bromomethyl)benzene, tetrabutylammonium bromide, CH_3CN, reflux.

Results and Discussion

Synthesis: Peptidomimetic cyclophanes **6–10** were prepared from a commercially available *N*-carbobenzyloxy protected amino acid following previously reported procedures (Scheme 1).[10] All compounds were purified by column chromatography and characterised by mass spectrometry as well as ^1H and ^{13}C NMR spectroscopy (see Supporting Information).[11]

Gelation behaviour: The gelation behaviour of compounds **6–10** was studied in a series of organic solvents. Typically, the desired amount of macrocycle was mixed with the solvent in a screw-capped vial, heated to the boiling temperature of the solvent, and left to cool by standing at room temperature. The formation of a gel was checked by turning the vial upside down. Transparent gels of different strength were formed in this manner (Table 1). The critical organogelator concentration was in the range of 0.3–0.5 wt % for all the aromatic solvents and 1 wt % in ethyl acetate. Gels were only formed by compounds **8b**, **8c**, **10b** and **10c** in the solvents studied, and none of the compounds jellified in either alcohols, THF, chloroform or dichloromethane. The T_g values of the resultant gels were determined by the "dropping-ball method" and were in the range of 35–40 °C.[12]

Table 1. Gelation behaviour of compounds **8**, **10b**, and **10c** in organic solvents.[a]

Solvent	8b	8c	10b	10c
benzene	G	G	G	wG
toluene	G	P	G	G
xylene	G	P	G	wG
styrene	G	–	wG	wG
anisole	G	G	wG	wG
nitrobenzene	G	G	wG	S
EtOAc	G	P	wG	wG

[a] G: gel; wG: weak gel; S: soluble; P: precipitate.

At first glance it was rather surprising to find that only four of the studied compounds formed gels despite the close structural resemblance among them. Several factors need to be taken into account in the study of the relationship between the molecular structure and the gelation behaviour of these compounds and include: 1) the amino acid residues utilised; 2) the length of the aliphatic spacer that separates the two amide groups; 3) the macrocyclic nature of the gelator; and general factors such as 4) the solvent; and 5) the cooling rate.

1) As can be seen in Table 1, compounds **8b**, **8c**, **10b** and **10c**, which are derived from natural β-methyl substituted amino acids L-valine and L-isoleucine, form gels in aromatic solvents and ethyl acetate. In contrast, compounds **9a** and **9c**, which contain isobutyl fragments derived from L-leucine, with a methyl group in the γ position, do not form gels in aromatic solvents. Instead, they are either soluble or precipitate out of solution; this is dependent on the polarity of the solvent. In general, compounds derived from L-alanine and L-glycine are only slightly soluble in aromatic solvents.
2) Compounds **8a** and **10a**, which bear only two methylene groups as aliphatic spacers, do not form gels.
3) The macrocyclic structure plays an important role in the gelation properties of these compounds. This has been demonstrated by preparing compound **11b**, which is an open chain benzylated analogue of **8b**, as it does not form gels in any of the studied organic solvents. Substitution of the aromatic moiety is also a determining factor. For example, when the *m*-phenylene unit in **8b** is replaced by a *p*-phenylene (**12b**), or a 1,4-naphthylidene (**13b**) fragment, gels do not form.
4) Gels are formed only in low polarity solvents. For example, gels are not formed when the solvent is an alcohol, indicating that hydrogen bonding may play an important part in the gelation behaviour of these compounds.
5) Transparent gels are formed when the hot solutions are left to spontaneously cool to room temperature or when they are cooled to 0 °C in an ice bath. However, when a 0.5 wt % weight solution of compound **8b** in benzene was cooled at a constant rate of 0.5 °C min^{-1} in a thermostatted bath, a fibrilar coagulated precipitate appeared at 50 °C rather than a gel.

Electron microscopy: The microscopic structure of the organogels formed by compounds **8b**, **8c**, **10b** and **10c** was studied by scanning electron microscopy. In every case, an entangled network of fibres of up to 100 μm length was observed. A closer look revealed that some of these fibres had an helicoidal shape, especially in the gels formed by compounds **8b** and **10b** in benzene. As can be seen in Figure 1, compounds **8b** and **10b** form right-handed helicoidal fibres of about 8 μm pitch and 1.5 μm width. Whereas helices coiled into larger fibres were observed if cooling was accomplished by standing at room temperature, an increase in the number of isolated helices together with a decrease in their dimensions was found when a gel of **8b** in benzene was formed by cooling the solution quickly in an ice bath. Simi-

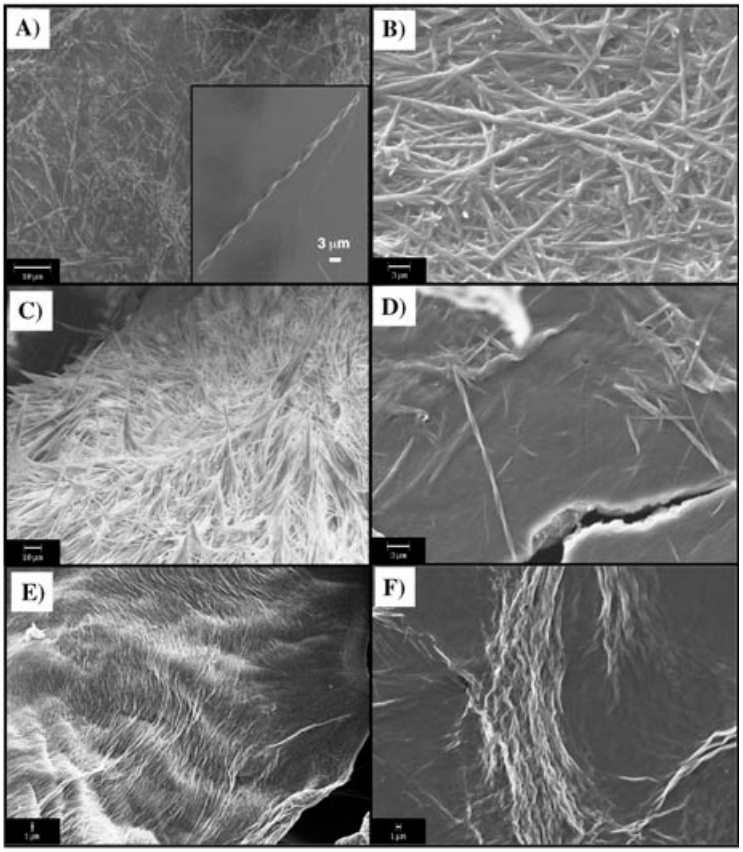

Figure 1. Scanning electron micrographs of the gels formed by: compound **8b** in benzene (A), styrene (B), and nitrobenzene (C); by compound **10b** in benzene (D); and by compound **10c** in benzene (E) and ethyl acetate (F).

haviour of compounds **6–10**, we conducted a detailed study of the conformational features of those compounds. For this purpose, analysis of data from X-ray diffraction, NMR spectroscopy, and molecular modelling was very helpful. Molecular mechanics calculations for compounds **6–10** were performed,[13] and the results revealed a high conformational variabiblity. Several features such as torsional angles involving the amide and amine groups, the relative disposition of the aromatic unit, as well as the presence of intramolecular hydrogen bonds were very sensitive to subtle structural modifications.

Especially interesting is the variability of the torsional angles in which the amide groups are involved, as they are the most likely to be involved in hydrogen bonding interactions in the supramolecular aggregates. For example, compound **9b** shows a lowest

lar, but less defined twisted fibres were observed in toluene, styrene, xylene, anisol, and ethyl acetate gels, while in nitrobenzene only straight fibres were found. On the other hand, as noted above, the slow cooling of a 0.5–2.0 wt% hot solution of compound **8b** in benzene at 0.5 °C min^{-1} in a thermostatted bath led to the precipitation of the gelator. For the most concentrated solutions (2 wt%), a coagulated gel (coagel) was formed at about 50 °C. Scanning electron micrographs revealed a network of straight fibres of several micrometer length in which expression of chirality had not occurred (see Supporting Information).

CD spectroscopy: To obtain information on the chirality of the organogel formed by compound **8b** in benzene, circular dichroism (CD) spectra were recorded at different temperatures during the gelation process, and an aggregation-induced increase on the CD signal was observed. As can be seen in Figure 2, formation of the organogel was accompanied by an increase in the negative CD band centred at about 277 nm. As clear exciton-coupling bands were not found, we could not obtain any further information on the supramolecular chirality of the gel. Similar results were found in other solvents such as ethyl acetate and dichloromethane.

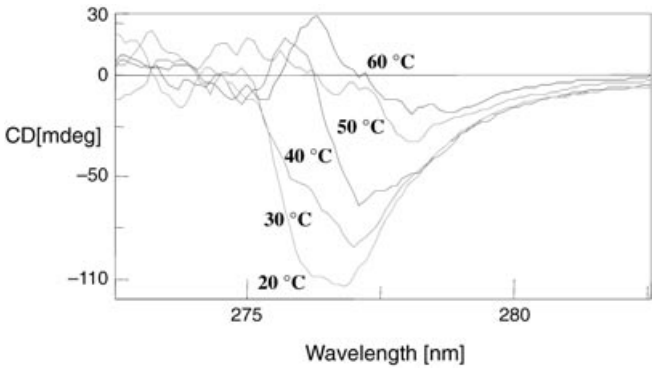

Figure 2. Temperature variable CD spectra of compound **8b** in benzene.

Structural studies: To understand the large influence that small changes in molecular structure had on the gelation be-

energy conformation in which the O=C−C_α−H torsional angles are both in a *syn*-type conformation (0.3°, 16.7°) and one C=O group is intramolecularly hydrogen bonded to an amine and an amide N−H. However, the lowest energy conformation found for the closely related compound **8b** is remarkably different. In particular, the above mentioned torsional angles are in an *anti*-type disposition (−124.9°, −157.2°) and only one intramolecular hydrogen bond is found (Figure 3). Moreover, structures that differed significantly from the global minimum were found in a narrow energy range (< 5 kJ mol^{-1}), and molecular dynamic simulations showed that these structures could easily be intercon-

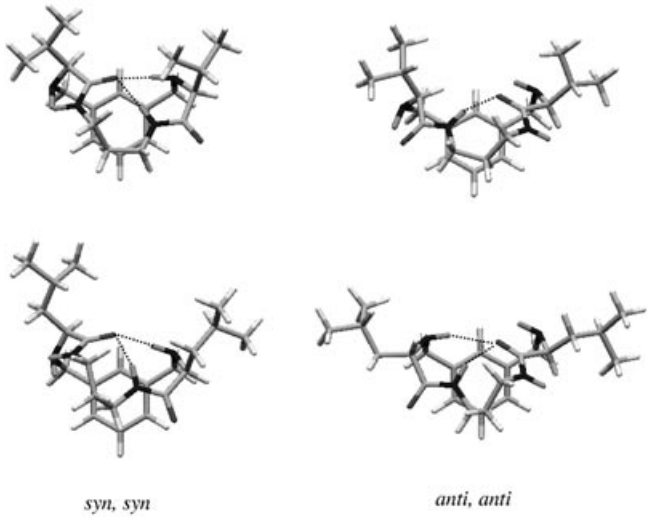

Figure 3. Calculated structures for compounds **8b** (top) and **9b** (bottom).

verted. For example, conformations with both O=C–C_α–H torsional angles in a *syn*-type disposition as well as in an *anti*-type were found within a 1 kJ mol^{-1} range for compound **9b**, and within a 3 kJ mol^{-1} range for compound **8b**. The flexibility of these macrocycles is consistent with the different self-assembling properties they display upon small structural variations. These variations could shift the conformational preferences of the different molecules and influence the efficiency of the aggregation processes.

Although the best approach toward understanding the fibre structure at the molecular level is by studying single crystals of the organogelator in the gel medium, this is only possible in a limited number of cases.[14] However, if one considers gelation as an incomplete crystallisation, it is feasible that in some cases a subtle change in the crystallisation conditions or a small structural modification may lead to single crystals that are suitable for X-ray diffraction studies. With this information, and keeping in mind that aggregate assembly in the gel and solid state may be different, it is possible to propose a model for the manner in which the molecules pack into fibres. Although in our studies we were not able to obtain single crystals for compounds **8b**, **8c**, **10b** or **10c** in any of the solvents in which they formed gels, we were able to grow single crystals of the closely related compounds **6c**, **7c**, **9a**, **9b** and **13b**. It should be noted that the crystal structures of compounds **8a** and **12a** in dichloromethane have recently been reported.[10,15]

Compound **6c** crystallises in benzene in the orthorhombic crystal system and $Pna2_1$ space group. Each molecule is connected to their neighbours by multiple hydrogen bonds that form a three-dimensional network (Figure 4). Poorly directional intramolecular hydrogen bonds with distances of 2.2–2.4 Å are found between the amide N–H and the amine nitrogen lone pairs.[16]

Compound **7c** crystallises in the monoclinic crystal system and $P2_1$ space group. In this case, molecules are assembled into columns by four hydrogen bonds between the amide groups (C=O···H–N amide) with distances of about 2.1 Å. The anti-parallel orientation of the amide groups favours

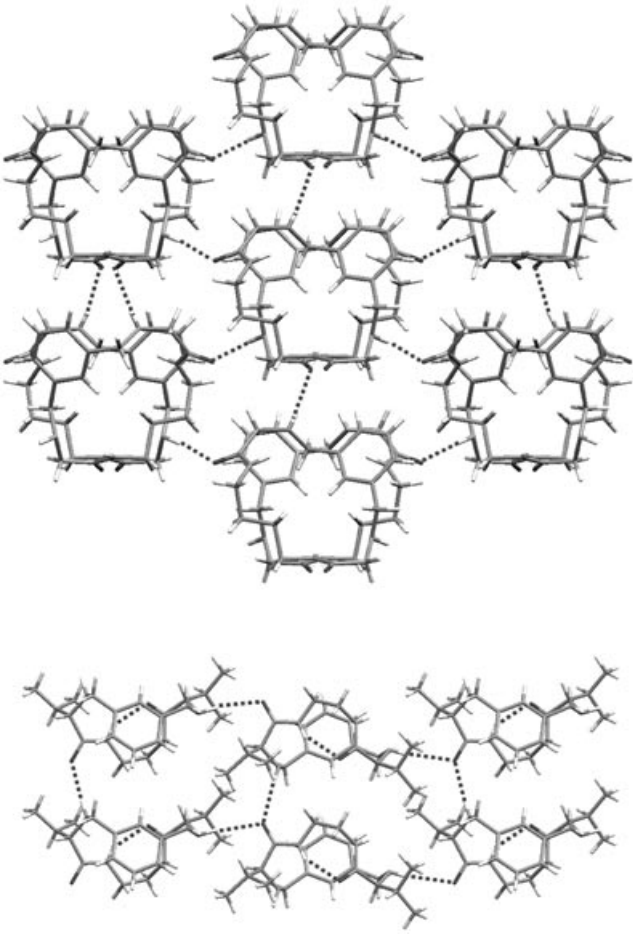

Figure 4. Three-dimensional packing found in the crystal structures of compounds **6c** (top) and **8a** (bottom).

the construction of a one-dimensional hydrogen-bonded network in which the intercolumnar packing is achieved through van der Waals interactions (Figure 5A).

Compound **9a** crystallises in the monoclinic crystal system and $P2_1$ space group. A columnar hydrogen bond assembly is also formed, but as can be seen in Figure 5B, two different parallel arrays of hydrogen bonds are present. One of them is formed by an interaction between an amide C=O group and an amide N–H of a neighbouring molecule (2.17 Å, 158.4°), while the other hydrogen-bonded chain comes from an interaction between the second amide C=O group, which is disposed in a slightly tilted parallel orientation to the first one, and an amine N–H group of the vicinal molecule (2.35 Å, 159.5°). The intercolumnar packing arises from van der Waals interactions between the leucine side chains, and the contact distances of about 4 Å are similar to those found in examples reported for some natural and synthetic leucine-containing peptides.[17]

Compound **9b** crystallises in benzene in the triclinic crystal system and $P1$ space group. The unit cell is composed of two molecules that correspond to two different conformers of **9b**, and displays five intermolecular N–H···O=C hydrogen bonds per molecule that have distances in the range of 1.9–2.2 Å (Figure 5C and 6). The crystal packing reveals a columnar assembly through hydrogen bonds and an interco-

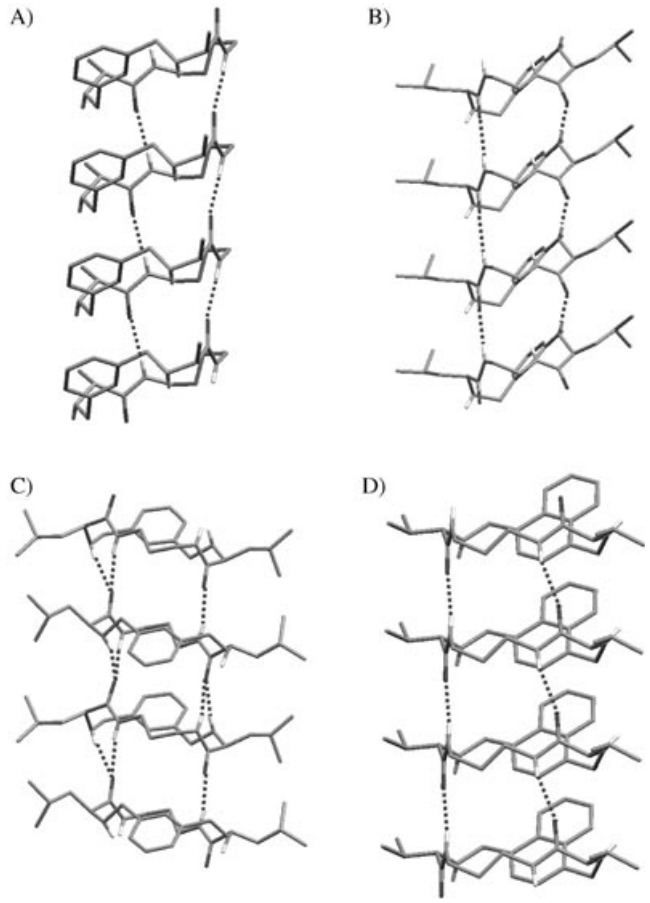

Figure 5. Columnar arrangement found in the crystal structures of compounds **7c** (A), **9a** (B), **9b** (C), and **13b** (D). Carbon-bound hydrogen atoms have been omitted for clarity.

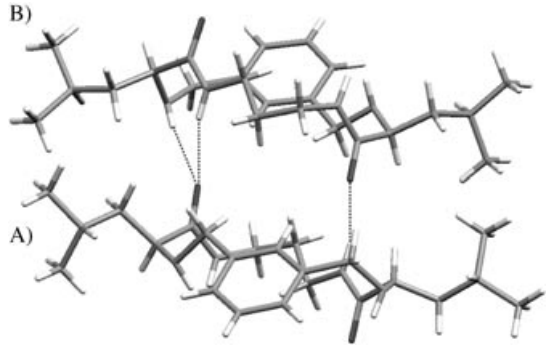

Figure 6. X-ray single crystal structure of compound **9b**. Two different conformers (A and B) are found in the unit cell.

lumnar assembly through cooperative van der Waals interactions (Figure 5C). The anti-parallel orientation of the amide groups favours the construction of a one-dimensional hydrogen-bonded network in which the leucine side chains are orthogonal to the column axis. The intercolumnar packing is similar to that found in **9a**, whereby the inter-residue distances are relatively short (ca. 3.8 Å).

Compound **13b** crystallises in chloroform in the monoclinic crystal system and $P2_1$ space group. The amide groups are in an anti-parallel arrangement and form a columnar hydrogen-bonded array. Two intermolecular hydrogen bonds arise between the C=O group and the amide N–H of a neighbouring molecule (2.06 and 2.26 Å). The aromatic fragments are stacked parallel to each other at a distance of about 3.6 Å (Figure 5D).

The conformations found in the crystal structures are in agreement with the conformational variability determined by the previously described molecular mechanics calculations. For example, compound **9b** contains two different conformers in its unit cell. One displays two *anti*-type O=C–C_α–H torsional angles (conformer A, Figure 6), while the other one contains two *syn*-type angles (conformer B, Figure 6).

A comparison of the crystal packing in these structures revealed significant differences. These were found to be dependent on both the nature of the amino acid residue and the length of the aliphatic spacer. Thus, the crystal structure of compound **6c**, which was derived from amino acid L-glycine (R = H), shows a three-dimensional packing through hydrogen bonding, whereas compound **7c**, which was derived from L-alanine (R = CH_3), stacks into columns with a one-dimensional hydrogen-bonded network in which additional intercolumnar van der Waals interactions are responsible for the final structure. In the latter compound, intercolumnar hydrogen bonds were not found probably because of steric effects associated with the presence of an α-methyl group. Compounds **9a** and **9b**, which are derived from L-leucine (R = $CH_2CH(CH_3)_2$), also form a columnar, one-dimensional hydrogen-bonded network similar to compound **7c**. In contrast, the length of the aliphatic spacer appears to influence the crystal structure of compounds **8a** and **9a**. An ethylenic spacer increases the rigidity of the ring system and leads to the formation of strong intramolecular hydrogen bonds. In compound **9a** columnar packing is still maintained, but in compound **8a**, which was derived from L-valine (R = $CH(CH_3)_2$), the presence of multiple intramolecular hydrogen bonds prevents the formation of columns and leads to a two-dimensional hydrogen-bonded arrangement. It appears that both factors, namely the higher accessibility of the hydrogen bonding centres in **6c**, and the presence of groups that introduce strain in the ring system in **8a** (shorter spacer length, β-methyl substituent) are responsible for their non-columnar packing.

As we were not able to obtain single crystals for organogelators **8b**, **8c**, **10b** or **10c**, X-ray powder diffraction experiments were used to investigate their xerogels and precipitates (Figure 7 and 8). From the results it can be seen that they are polycrystalline, as there is a high degree of order inside the fibres. Moreover, as already revealed from the electron microscopy studies, the solvent used and the cooling rate also influence the observed diffraction patterns. For example, a similar diffractogram was obtained for xerogels of compound **8b** in benzene and ethyl acetate, in contrast with that of the xerogel formed in nitrobenzene. It should also be noted that the diffraction pattern of the precipitate obtained by slow cooling of **8b** in benzene was different to that of the xerogel of **8b**. The former is similar to the one obtained for compound **9b** when the solid was precipitated under the same conditions, and is therefore, in agreement

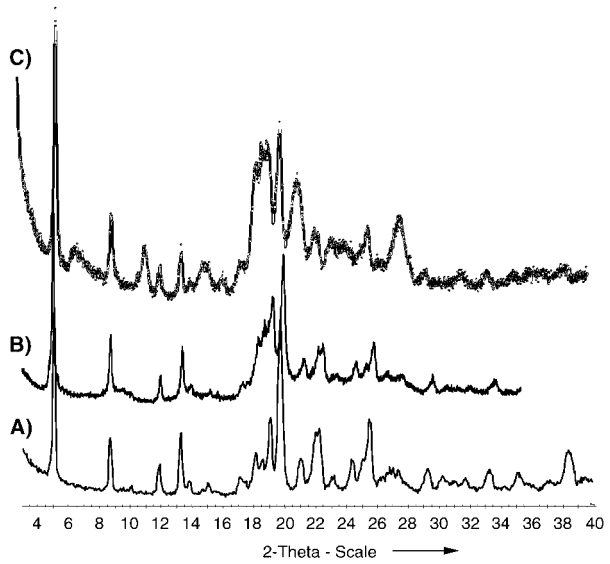

Figure 7. X-ray powder diffraction of the xerogels obtained for **8b** (A) and **10b** (B) in benzene, and **8b** (C) in ethyl acetate.

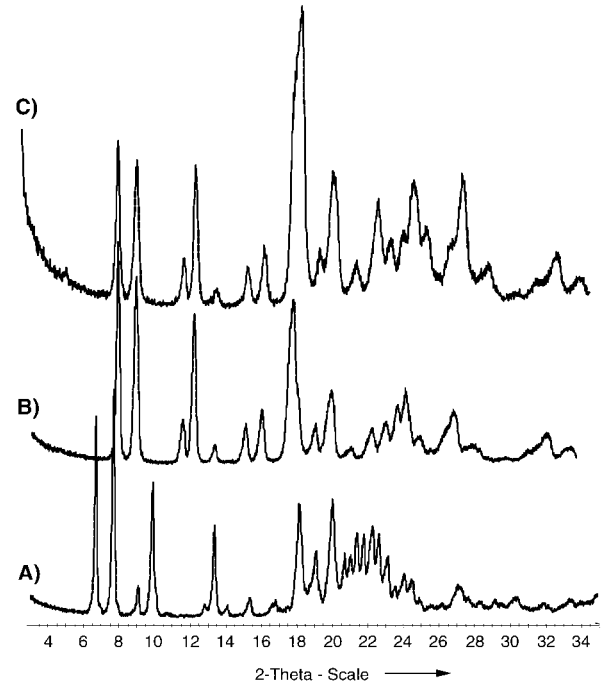

Figure 8. X-ray powder diffraction of the solids obtained for **9b** (A) and **8b** (B) after slow precipitation in benzene, and the xerogel from **8b** in nitrobenzene (C).

with the microscopic structure described above. This suggests that compound **8b** has at least two different packing modes at the supramolecular level, and that these lead to the two different diffraction patterns shown in Figure 7 and 8, respectively. The diffraction peaks shown in Figure 8A are in agreement with those obtained after the single crystal structure simulation of compound **9b**, and thus, correspond to a similar columnar arrangement of molecules. On the other hand, the diffraction patterns displayed by the xerogels in Figure 7 show three sharp reflections at 17.7, 10.2, and 6.7 Å, corresponding to the (10), (11) and (21) reflections of a columnar hexagonal packing. This difference in packing could explain their different aggregation behaviour.

The results infer two possible conclusions. Firstly, it could be argued that the molecular conformation of **8b** is different in the precipitate and gel. Although it is not possible to completely discard this hypothesis, NMR data suggest that this is not the case. In particular, the ^{1}H NMR spectra of the gel formed by **8b** in [D_6]benzene at both 30 and 50 °C are almost identical (aside from the shift in the amide signal), suggesting that the conformational preference does not significantly change within this temperature range.[18] In view of this, it could be argued that although the molecules initially have the same conformation, they form superaggregates in different ways. As a result, a gel is formed at 20 °C, while a polycrystalline precipitate occurs at 50 °C. This explanation is perfectly reasonable if one considers gelation to be a supramolecular polymerisation in which the main difference at 20 and 50 °C is the length of the supramolecular aggregates formed. Indeed, NOE measurements obtained by irradiation of the amide resonance showed positive enhancements at 50 °C but negative ones for the gels at 20 °C. This behaviour is the result of the increased correlation times obtained upon aggregation and, accordingly, as pointed out previously by Feringa and co-workers, the average molecular weight is expected to be at least around 1500, which in our case is in accordance with the presence of tetramers or larger aggregates in solution.[2i] In the studied case it seems that by slow cooling, at 50 °C the molecules superaggregate in a crystalline way that results in precipitation and that the faster cooling till 20 °C leads to aggregates long enough to drive the system towards a columnar hexagonal packing that forms the fibres of the gel. These two packing modes have a dramatic effect on the shapes observed by electron microscopy. In one case, straight fibres are observed, while in the other case, helices arise.

The diffractogram of a dried gel of **8b** obtained from nitrobenzene was very similar to that obtained from the precipitate of the same compound in benzene. This solvent probably represents a borderline situation in that the self-assembly interactions are strong enough to promote physical gelation, but the seminal supramolecular aggregates are not long enough to yield the hexagonal superaggregation mode.

The above results can subsequently be used to provide a tentative model for the supramolecular arrangement of compounds **8b**, **8c**, **10b** and **10c** that leads to gel formation. It is generally accepted that the formation of one-dimensional assemblies is an essential requirement for the obtention of long fibres. In our case it seems reasonable that compounds **8b**, **8c**, **10b** and **10c** could assemble into columns in a manner that is similar to the way that their crystalline analogues form. Furthermore, IR and NMR spectroscopy confirm the formation of strong hydrogen bonds during the gelation process. As can be seen in Figure 9, the gelation process for compound **8b** is accompanied by an increase in the associated N–H stretching peaks at 3330 and 3310 cm^{-1}, the appearance of a shifted C=O (amide I) band at 1625–1635 cm^{-1}, and a decrease in the initial C=O band at 1680 cm^{-1}. On the other hand, the ^{1}H NMR spectra show a

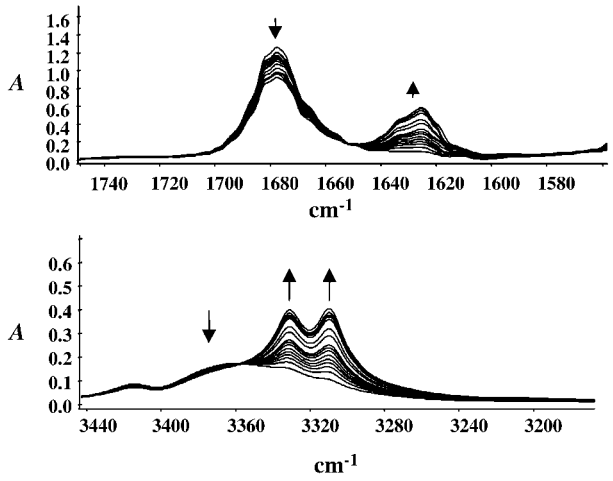

Figure 9. IR spectra collected during the gelation process of the N–H stretching region (top) and C=O stretching amide I band (bottom) of compound **8b** in benzene. Arrows indicate the evolution of the band upon gelation.

downfield shift of the amide hydrogen signal upon gelation (not shown). All the data concur with the observations that gel formation does not occur in polar solvents because the hydrogen-bond interactions are less intense.

To gain information about molecular arrangement in the supramolecular aggregates it is valuable to know the conformation of the molecules in solution. NOE experiments were particularly helpful in identifying the presence of conformations with *syn*-type or *anti*-type O=C–C_α–H torsion angles. It should be noted that in the *anti*-type conformations the amide hydrogen atom and the proton attached to the chiral carbon atom are in close proximity. As a result, the NOEs between these two protons should be greater than those observed for the *syn*-type conformations. Indeed, this was confirmed by the NOE enhancements observed for compounds **8a**, **12a** and **13b** upon irradiation of the amide protons.[19] The crystal structures of these three compounds showed that **12a** contains one *anti*-type and one *syn*-type O=C–C_α–H dihedral angle, that in **8a** these angles have a *syn*-type disposition, while in **13b** both are *anti*-type angles. It can be seen in Table 2 that the measured NOE enhancements correlate well with the O=C–C_α–H dihedral angles present in

Table 2. Dihedral angle O=C–C_α–H and H_α···HN distances versus NOE at 50 °C.

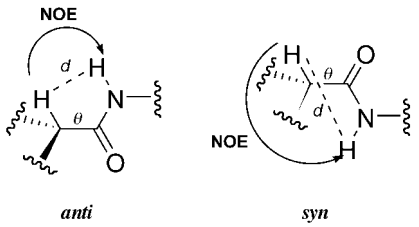

Compound	θ [°]	Distance [d] H···HN [Å]	NOE [%]
8a	30.42, 41.55	3.29, 3.25	1.9
12a	65.90, −172.10	3.07, 2.17	3.4
13b	−172.08, 177.40	2.18, 2.22	2.9
8b[a]	128.5, −158.6	2.47, 2.27	3.1
8c[a]	−4.7, 12.7	3.57, 3.61	1.7
10b[a]	135.7, −170.9	2.38, 2.20	3.2

[a] Values determined from model structures.

the different structures. In particular, they were around 3% for those molecules with *anti*-type conformations and less than 2% in the *syn*-type conformations. When compounds **8b** and **10b**, which behave as organogelators in benzene were studied, NOE enhancements higher than 3% were measured. This strongly suggests that *anti*-type dihedral angles are present in these compounds.

Altogether, these data support the hypothesis that conformations such as conformer A in crystal structure of **9b** (Figure 6) are the main constituents present for compounds **8b** and **10b** in benzene. This is also in agreement with the conformation found in the crystal structure of the valine derivative **13b**. Most likely, the formation of aggregates from these type of conformers should be responsible for the gel formation. Indeed, as can be seen in Figure 10A, a mini-

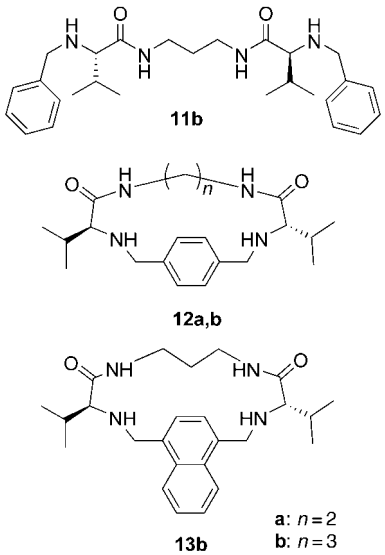

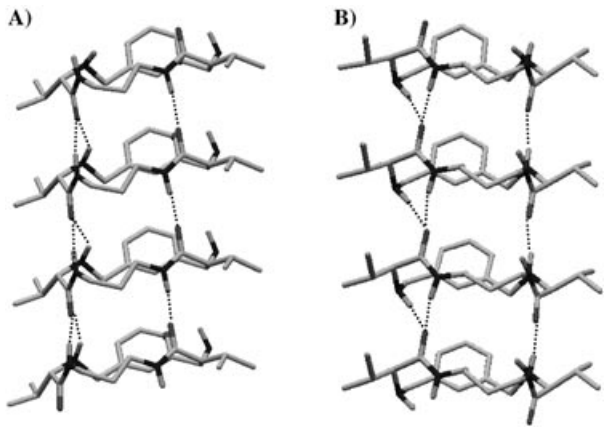

Figure 10. Calculated model for the columnar arrangement of **8b** (A) and **8c** (B). Hydrogen atoms bonded to carbon atoms have been omitted for clarity.

mum energy structure corresponding to a columnar packing structure can be built from the mentioned conformations. It should be noted that each molecule participates in six hydrogen bonds that hold the structure together. Similar studies were carried out for compounds **8c** and **10c**. The data obtained indicates that both torsional angles have a *syn*-type disposition such as that shown in conformer B in the crystal structure of **9b** (Figure 6). A model for the packing of compound **8c** is also proposed in Figure 10B.

It should be noted that compounds **7c**, **9a**, **9b** and **13b**, which are capable of self-assembly into columns as occurs in their respective crystal structures do not gel. Structural differences, which lead to conformations that self-assemble less efficiently, most likely explain why these compounds behave differently than the organogelators. The NOE measurements described above concur with this fact. In particular, negative NOEs (and large aggregates) were only observed for the compounds that form gels. In the case of **13b** it seems that the presence of a 1,4-disubstituted aromatic spacer makes the molecule rigid in such a way that only four hydrogen bonds per molecule can be formed in the supramolecular aggregates. For compounds **7c** and **9a**, the presence of an alanine residue in the former, a shorter aliphatic spacer in the latter, produces conformations that also self-assemble by means of only four hydrogen bonds per unit. It is interesting that compound **9b**, which forms columnar aggregates through seven hydrogen bonds per molecule in the crystal structure does not gel. In this case, the coexistence of two different conformers in the supramolecular aggregate introduces an entropically unfavourable factor that overcomes the favourable enthalpic contribution of the hydrogen bonds. These results clearly identify the two requisites in order for physical gelation to take place, namely the formation of aggregates in a preferred direction (columns) and the presence of strong intermolecular interactions.

Conclusion

The self-assembly behaviour of small peptidomimetic cyclophanes **6**–**10** in organic solvents has been studied in detail. The transcription of molecular chirality into the supramolecular level has been revealed by scanning electron microscopy. As can be seen by the fact that only four of the 15 compounds considered actually form gels, the self-assembly of such compounds is very sensitive to small structural changes such as the nature of the amino acid residue or aromatic moiety, and the length of the aliphatic spacer. These factors have an important influence on the conformational preferences of these types of molecules, as well as on their supramolecular self-assembly. Other factors such as cooling rate and solvent have been shown to determine the microscopic shape of the aggregates. All the results indicate that the strength of the interaction between organogelator molecules is the key factor that determines the average length of the aggregates at a given temperature and their further superaggregation. Upon consideration of all the results, models for the assembly of the organogels have been proposed.

Experimental Section

NMR spectroscopy: The NMR experiments were carried out either on a Varian INOVA 500 spectrometer (500 MHz for ^{1}H and 125 MHz for ^{13}C) or a Varian MERCURY 300 spectrometer (300 MHz for ^{1}H and 75 MHz for ^{13}C). Chemical shifts are reported in ppm from tetramethylsilane with the solvent resonance as the internal standard.

Mass spectrometry: Mass spectra were recorded on a Micromass Quattro LC spectrometer equipped with an electrospray ionisation source and a triple-quadrupole analyzer.

Molecular modelling: MonteCarlo conformational searches and molecular dynamics studies were performed with MACROMODEL 7.0[20a] using AMBER*[20b] as the force field and GB/SA[20c] simulation of chloroform as solvent. The MonteCarlo conformational search involved modification of the torsional angles automatically set-up by the program. One thousand step cycles departing from different conformers in each case were performed until convergence was found. Molecular dynamics calculations were carried out using the following conditions: simulation temperature = 300 K; and length of simulation = 5 ns with 1.5 fs steps. SHAKE[20d] was used to constrain the length of bonds to hydrogen.

X-ray powder diffraction: Data collection was performed at room temperature on a Siemens D5000 diffractometer using $Cu_{K\alpha}$ radiation. Samples of the powdered solids were placed on a quartz sample holder and data were collected for 2θ values between 3 and 35° with a step size of 0.05° and a time step of 20 s.

X-ray single crystal diffraction: Data collection was performed at room temperature on a Siemens Smart CCD 1 K diffractometer using graphite monochromated $Mo_{K\alpha}$ radiation ($\lambda = 0.71073$ Å) with a nominal crystal-to-detector distance of 4.0 cm. A hemisphere of data was collected based on three ω-scan runs (starting $\omega = -28°$) at values $\phi = 0$, 90, and 180 with the detector at $2\theta = 28°$. In each of these runs, frames (606, 435 and 230, respectively) were collected at 0.3° intervals and 40 s per frame. The diffraction frames were integrated using the SAINT package[21a] and corrected for absorption with SADABS.[21b] Structure solution was performed with SHELXTL[21c] and refinement on F^2 was done with SHELXL-97.[21d] The illustrations shown in Figure 3, 4, and 5 were prepared with MERCURY.[21e]

Electron microscopy: Scanning electron micrographs were taken on a LEO 440I microscope equipped with a digital camera. Samples of the xerogels were prepared by placing the gel on top of a tin plate, and after slow drying of the solvent they were sputtered with Au/Pd in a Polaron SC7610 Sputter Coater from Fisons Instruments.

CD spectroscopy: CD spectra were recorded on a Jasco J-810 spectropolarimeter. The gel samples were prepared in a quartz cuvette of 1 cm path length and the measurement temperature was varied from 20 to 60 °C.

Syntheses: The *N*-hydroxysuccinimide esters of the amino acids, the *N*,*N*′-bis(*N*-Cbz-L-aminoacyl)diamines, the *N*,*N*′-bis(L-aminoacyl)diamines (**1**–**5**, **a**–**c**), and the macrocycles (**6**–**10**, **a**–**c**, and **13b**) were prepared following previously reported procedures.[7]

Compound CBz-1a: Yield: 89%; ^{1}H NMR (500 MHz, [D$_6$]DMSO): $\delta =$ 7.88 (br s, 2H), 7.35 (m, 10H), 7.32 (br s, 2H), 5.03 (s, 4H), 3.58 (m, 4H), 3.12 ppm (m, 4H); ^{13}C NMR (125 MHz, [D$_6$]DMSO): $\delta = 170.0$, 157.2, 137.7, 129.0, 128.5, 66.2, 44.3, 39.0 ppm; IR (KBr): $\tilde{\nu} = 3320$, 3033, 1987, 1642, 1535 cm^{-1}; MS (ESI): *m/z* (%): 465.6 $[M+Na]^+$; elemental analysis calcd (%) for $C_{22}H_{26}N_4O_6$: C 59.72, H 5.92, N 12.66; found: C 59.93, H 6.48, N 12.64.

Compound CBz-1b: Yield: 76%; ^{1}H NMR (500 MHz, [D$_6$]DMSO): $\delta =$ 7.84 (m, 2H), 7.41 (m, 2H), 7.35–7.30 (m, 10H), 5.03 (s, 4H), 3.58 (m, 4H), 3.06 (m, 4H), 1.51 ppm (m, 2H); ^{13}C NMR (125 MHz, [D$_6$]DMSO): $\delta = 169.2$, 156.6, 137.0, 128.4, 127.9, 127.8, 65.6, 43.6, 36.2, 29.2 ppm; IR (KBr): $\tilde{\nu} = 3320$, 3038, 1687, 1646, 1534 cm^{-1}; MS (ESI): *m/z*: 479.6 $[M+Na]^+$; elemental analysis calcd (%) for $C_{23}H_{28}N_4O_6$: C 60.52, H 6.18, N 12.27; found: C 61.05, H 6.88, N 12.36.

Compound CBz-1c: Yield: 91%; ^{1}H NMR (300 MHz, $CDCl_3$): $\delta = 7.67$ (br s, 2H), 7.30 (m, 12H), 5.02 (s, 4H), 3.57 (m, 4H), 3.04 (m, 4H), 1.38 ppm (m, 4H); ^{13}C NMR (75 MHz, $CDCl_3$): $\delta = 168.9$, 156.6, 137.2, 128.4, 127.84, 127.75, 62.8, 44.0, 38.6, 26.9 ppm; IR (KBr): $\tilde{\nu} = 3317$, 3031, 1684, 1640, 1531 cm^{-1}; MS (ESI): *m/z*: 471.3 $[M+H]^+$, 493.3 $[M+Na]^+$,

509.3 $[M+K]^+$; elemental analysis calcd (%) for $C_{24}H_{30}N_4O_6$: C 61.26, H 6.43, N 11.91; found: C 61.47, H 7.02, N 12.09.

Compound CBz-2a: Yield: 98%; $[\alpha]_D^{20}=+14.5$ ($c=0.025$ in $CHCl_3$/CH_3OH, 7:3 v/v); ^1H NMR (300 MHz, $CDCl_3$): $\delta=7.31$ (m, 10H), 6.73 (brs, 2H), 5.54 (m, 2H), 5.07 (m, 4H), 4.17 (m, 2H), 3.47 (m, 2H), 3.24 (m, 2H), 1.34 ppm (d, $J=6.8$ Hz, 6H); ^{13}C NMR (125 MHz, $CDCl_3$): $\delta=$ 173.9, 156.2, 135.9, 128.0, 127.7, 127.5, 66.5, 50.4, 38.5, 17.5 ppm; IR (KBr): $\tilde{\nu}=3313$, 3091, 3033, 1687, 1656, 1538 cm^{-1}; MS (ESI): m/z: 493.7 $[M+Na]^+$; elemental analysis calcd (%) for $C_{24}H_{30}N_4O_6$: C 61.26, H 6.43, N 11.91; found: C 61.49, H 6.91, N 11.94.

Compound CBz-2b: Yield: 89%; $[\alpha]_D^{20}=-2.7$ ($c=0.025$ in $CHCl_3$/CH_3OH, 7:3 v/v); ^1H NMR (300 MHz, $CDCl_3$): $\delta=7.34$ (m, 10H), 6.83 (brs, 2H), 5.37 (m, 2H), 5.10 (m, 4H), 4.19 (m, 2H), 3.40 (m, 2H), 3.15 (m, 2H), 1.60 (m, 2H), 1.37 ppm (d, $J=6.8$ Hz, 6H); ^{13}C NMR (75 MHz, $CDCl_3$): $\delta=173.7$, 156.2, 135.9, 128.1, 127.7, 127.5, 66.5, 50.4, 36.0, 28.2, 17.7 ppm; IR (KBr): $\tilde{\nu}=3302$, 3066, 1690, 1644, 1555, 1535 cm^{-1}; MS (ESI): m/z: 507.7 $[M+Na]^+$; elemental analysis calcd (%) for $C_{25}H_{32}N_4O_6$: C 61.97, H 6.66, N 11.56; found: C 62.19, H 7.28, N 11.59.

Compound CBz-2c: Yield: 88%; ^1H NMR (300 MHz, $CDCl_3$): $\delta=7.33$ (m, 10H), 6.63 (brs, 2H), 5.54 (m, 2H), 5.07 (m, 4H), 4.26 (m, 2H), 3.32 (m, 2H), 3.09 (m, 2H), 1.44 (m, 4H), 1.36 ppm (d, $J=7.3$ Hz, 6H); ^{13}C NMR (75 MHz, $CDCl_3$): $\delta=173.4$, 156.1, 135.9, 128.1, 127.7, 127.5, 66.5, 50.2, 38.5, 25.8, 17.9 ppm; IR (KBr): $\tilde{\nu}=3303$, 3105, 3058, 1690, 1647, 1536 cm^{-1}; MS (ESI): m/z: 521.8 $[M+Na]^+$; elemental analysis calcd (%) for $C_{26}H_{34}N_4O_6$: C 62.63, H 6.87, N 11.24; found: C 62.98, H 7.43, N 11.35.

Compound CBz-4a: Yield: 88%; $[\alpha]_D^{20}=+20.7$ ($c=0.025$ in $CHCl_3$/CH_3OH, 9:1 v/v); ^1H NMR (300 MHz, $[D_6]$DMSO): $\delta=7.94$ (brs, 2H), 7.34 (m, 12H), 5.00 (m, 4H), 3.95 (m, 2H), 3.07 (m, 4H), 1.56 (m, 2H), 1.41 (m, 4H), 0.83 ppm (dd, $J=6.4$ and $J'=5.9$ Hz, 12H); ^{13}C NMR (75 MHz, $[D_6]$DMSO): $\delta=172.4$, 155.9, 137.0, 128.3, 127.7, 65.3, 53.1, 40.7, 38.2, 24.2, 24.1, 22.9, 21.4 ppm; IR (KBr): $\tilde{\nu}=3304$, 3092, 1687, 1650, 1534 cm^{-1}; MS (ESI): m/z: 556.0 $[M+H]^+$; elemental analysis calcd (%) for $C_{30}H_{42}N_4O_6$: C 64.96, H 7.63, N 10.10; found: C 65.23, H 8.29, N 10.18.

Compound CBz-4b: Yield: 89%; $[\alpha]_D^{20}=+4.9$ ($c=0.025$ in $CHCl_3$/CH_3OH, 9:1 v/v); ^1H NMR (300 MHz, $[D_6]$DMSO): $\delta=7.90$ (brs, 2H), 7.40 (m, 12H), 4.99 (m, 4H), 3.94 (m, 2H), 3.01 (m, 4H), 1.56 (m, 2H), 1.43 (m, 6H), 0.83 ppm (dd, $J=7.3$ and $J'=6.8$ Hz, 12H); ^{13}C NMR (75 MHz, $[D_6]$DMSO): $\delta=172.2$, 155.7, 137.0, 128.2, 127.7, 127.6, 65.3, 53.1, 40.7, 36.1, 29.1, 24.2, 22.9, 21.4 ppm; IR (KBr): $\tilde{\nu}=3298$, 3078, 1691, 1649, 1535 cm^{-1}; MS (ESI): m/z: 570.1 $[M+H]^+$; elemental analysis calcd (%) for $C_{31}H_{44}N_4O_6$: C 65.47, H 7.80, N 9.85; found: C 65.26, H 8.54, N 9.86.

Compound CBz-4c: Yield: 79%; $[\alpha]_D^{20}=-4.7$ ($c=0.025$ in $CHCl_3$/CH_3OH, 9:1 v/v); ^1H NMR (300 MHz, $[D_6]$DMSO): $\delta=7.88$ (brs, 2H), 7.32 (m, 12H), 4.99 (m, 4H), 3.95 (m, 2H), 3.00 (m, 4H), 1.55 (m, 2H), 1.33 (m, 8H), 0.83 ppm (dd, $J=6.8$ and $J'=6.4$ Hz, 12H); ^{13}C NMR (125 MHz, $[D_6]$DMSO): $\delta=172.9$, 156.6, 136.3, 128.5, 128.1, 127.9, 66.9, 53.6, 41.9, 38.9, 26.2, 24.8, 22.9, 21.1 ppm; IR (KBr): $\tilde{\nu}=3299$, 3077, 1683, 1650, 1532 cm^{-1}; MS (ESI): m/z: 584.1 $[M+H]^+$; elemental analysis calcd (%) for $C_{32}H_{46}N_4O_6$: C 65.96, H 7.96, N 9.61; found: C 65.78, H 8.75, N 9.57.

Compound CBz-5a: Yield: 88%; ^1H NMR (300 MHz, $[D_6]$DMSO): $\delta=$ 7.98 (brs, 2H), 7.28 (m, 12H), 5.00 (s, 4H), 3.76 (t, 2H), 3.07 (m, 4H), 1.65 (m, 2H), 1.40 (m, 2H), 1.05 (m, 2H), 0.77 ppm (m, 12H); ^{13}C NMR (75 MHz, $[D_6]$DMSO): $\delta=171.3$, 156.0, 137.0, 128.3, 127.7, 127.6, 65.3, 59.2, 38.1, 36.1, 24.4, 15.4, 10.9 ppm; IR (KBr): $\tilde{\nu}=3297$, 1690, 1645, 1541 cm^{-1}; MS (ESI): m/z: 555.9 $[M+H]^+$; elemental analysis calcd (%) for $C_{30}H_{42}N_4O_6$: C 64.96, H 7.63, N 10.10; found: C 65.38, H 8.14, N 10.21.

Compound CBz-5b: Yield: 88%; $[\alpha]_D^{20}=-0.6$ ($c=0.025$ in $CHCl_3$/CH_3OH, 7:3 v/v); ^1H NMR (300 MHz, $[D_6]$DMSO): $\delta=7.96$ (m, 2H), 7.34 (m, 12H), 5.01 (s, 4H), 3.79 (m, 2H), 3.05 (m, 4H), 1.68 (m, 2H), 1.51 (m, 2H), 1.41 (m, 2H), 1.10 (m, 2H), 0.80 ppm (m, 12H); ^{13}C NMR (75 MHz, $[D_6]$DMSO): $\delta=171.1$, 156.0, 137.0, 128.3, 127.7, 127.6, 65.3, 59.2, 36.2, 36.1, 29.0, 24.4, 15.3, 10.9 ppm; IR (KBr): $\tilde{\nu}=3293$, 3089, 1690, 1645, 1541 cm^{-1}; MS (ESI): m/z: 570.0 $[M+H]^+$; elemental analysis calcd (%) for $C_{31}H_{44}N_4O_6$: C 65.47, H 7.80, N 9.85; found: C 65.38, H 8.46, N 9.92.

Compound CBz-5c: Yield: 88%; $[\alpha]_D^{20}=-4.9$ ($c=0.026$ in $CHCl_3$/CH_3OH, 7:3 v/v); ^1H NMR (300 MHz, $[D_6]$DMSO): $\delta=7.96$ (brs, 2H), 7.34 (m, 12H), 5.02 (s, 4H), 3.80 (m, 2H), 3.03 (m, 4H), 1.65 (m, 2H), 1.37 (m, 6H), 1.08 (m, 2H), 0.78 ppm (m, 12H); ^{13}C NMR (75 MHz, $[D_6]$DMSO): $\delta=171.0$, 155.9, 137.1, 128.3, 127.7, 127.6, 65.3, 59.1, 38.1, 36.2, 26.4, 24.4, 15.3, 10.8 ppm; IR (KBr): $\tilde{\nu}=3295$, 3091, 1691, 1647, 1537 cm^{-1}; MS (ESI): m/z: 605.9 $[M+Na]^+$; elemental analysis calcd (%) for $C_{32}H_{46}N_4O_6$: C 65.96, H 7.96, N 9.61; found: C 65.44, H 8.52, N 9.22.

Compound 1a·2HBr: (hygroscopic) Yield: 78%; ^1H NMR (300 MHz, D_2O): $\delta=3.68$ (m, 4H), 3.28 ppm (m, 4H); ^{13}C NMR (75 MHz, D_2O): $\delta=167.3$, 40.5, 38.7 ppm; IR (KBr): $\tilde{\nu}=3362$, 3222, 3118, 1676, 1655, 1570, 1509 cm^{-1}; MS (ESI): m/z: 335.4 $[M+H\cdot Br_2]^+$.

Compound 1b·2HBr: (hygroscopic) Yield: 60%; ^1H NMR (300 MHz, D_2O): $\delta=3.68$ (s, 4H), 3.17 (t, 4H), 1.64 ppm (m, 2H); ^{13}C NMR (75 MHz, D_2O): $\delta=167.0$, 40.5, 36.7, 27.9 ppm; IR (KBr): $\tilde{\nu}=3257$, 2996, 1648, 1591, 1555 cm^{-1}; MS (ESI): m/z: 189.1 $[M+H]^+$.

Compound 1c·2HBr: (hygroscopic) Yield: 79%; ^1H NMR (300 MHz, D_2O): $\delta=3.66$ (s, 4H), 3.13 (m, 4H), 1.42 ppm (m, 4H); ^{13}C NMR (75 MHz, D_2O): $\delta=166.9$, 40.5, 39.1, 25.7 ppm; IR (KBr): $\tilde{\nu}=3243$, 3077, 3009, 1663, 1566 cm^{-1}; MS (ESI): m/z: 203.1 $[M+H]^+$.

Compound 2a·2HBr: (hygroscopic) Yield: 78%; $[\alpha]_D^{20}=+14.8$ ($c=0.025$ in CH_3OH/H_2O, 8:2 v/v); ^1H NMR (500 MHz, CD_3OD): $\delta=3.96$ (m, 2H), 3.37 (m, 4H), 1.50 ppm (d, $J=6.8$ Hz, 6H); ^{13}C NMR (75 MHz, D_2O): $\delta=171.0$, 49.2, 38.8, 16.6 ppm; IR (KBr): $\tilde{\nu}=3442$, 3078, 1676, 1561 cm^{-1}; MS (ESI): m/z: 225.1 $[M+Na]^+$.

Compound 2b·2HBr: (hygroscopic) Yield: 87%; $[\alpha]_D^{20}=+8.9$ ($c=0.025$ in CH_3OH/H_2O, 8:2 v/v); ^1H NMR (500 MHz, CD_3OD): $\delta=3.96$ (m, 2H), 3.29 (m, 4H), 1.77 (m, 2H), 1.51 ppm (d, $J=7.3$ Hz, 6H); ^{13}C NMR (125 MHz, CD_3OD): $\delta=171.1$, 50.4, 50.3, 37.9, 30.0, 17.7 ppm; IR (KBr): $\tilde{\nu}=3448$, 3252, 1671, 1561 cm^{-1}; MS (ESI): m/z: 217.2 $[M+H]^+$.

Compound 2c: Yield: 32%; $[\alpha]_D^{20}=-1.1$ ($c=0.025$ in $CHCl_3$); ^1H NMR (500 MHz, $CDCl_3$): $\delta=7.35$ (m, 2H), 3.48 (m, 2H), 3.27 (m, 4H), 1.55 (m, 4H), 1.48 (m, 4H), 1.32 ppm (d, $J=6.8$ Hz, 6H); ^{13}C NMR (125 MHz, $CDCl_3$): $\delta=175.7$, 50.8, 38.6, 27.1, 21.8 ppm; IR (KBr): 3281, 3084, 1648, 1554, 1535 cm^{-1}; MS (ESI): m/z: 231.4 $[M+H]^+$; elemental analysis calcd (%) for $C_{10}H_{22}N_4O_2$: C 52.15, H 9.63, N 24.33; found: C 52.38, H 9.81, N 24.27.

Compound 4a: Yield: 95%; $[\alpha]_D^{20}=-39.0$ ($c=0.025$ in $CHCl_3$); ^1H NMR (300 MHz, $CDCl_3$): $\delta=7.68$ (m, 2H), 3.38 (m, 6H), 1.69 (m, 4H), 1.41 (brs, 4H), 1.32 (m, 2H), 0.92 ppm (m, 12H); ^{13}C NMR (75 MHz, $CDCl_3$): $\delta=176.6$, 53.4, 44.0, 39.3, 24.7, 23.3, 21.2 ppm; IR (KBr): $\tilde{\nu}=$ 3361, 3278, 3189, 1653, 1609, 1555 cm^{-1}; MS (ESI): m/z: 287.2 $[M+H]^+$; elemental analysis calcd (%) for $C_{14}H_{30}N_4O_2$: C 58.71, H 10.56, N 19.56; found: C 59.05, H 11.26, N 19.31.

Compound 4b: Yield: 89%; $[\alpha]_D^{20}=-33.3$ ($c=0.025$ in $CHCl_3$); ^1H NMR (300 MHz, $CDCl_3$): $\delta=7.67$ (m, 2H), 3.37 (m, 2H), 3.25 (m, 4H), 1.66 (m, 6H), 1.55 (brs, 4H), 1.31 (m, 2H), 0.90 ppm (dd, $J=6.4$ and $J'=$ 8.8 Hz, 12H); ^{13}C NMR (125 MHz, $CDCl_3$): $\delta=175.8$, 53.5, 44.0, 35.7, 29.6, 24.8, 23.3, 21.4 ppm; IR (KBr): $\tilde{\nu}=3299$, 3073, 1652, 1532 cm^{-1}; MS (ESI): m/z: 339.8 $[M+K]^+$; elemental analysis calcd (%) for $C_{15}H_{32}N_4O_2$: C 59.97, H 10.74, N 18.65; found: C 60.13, H 10.98, N 18.71.

Compound 4c: Yield: 79%; $[\alpha]_D^{20}=-35.8$ ($c=0.025$ in $CHCl_3$); ^1H NMR (300 MHz, $CDCl_3$): $\delta=7.40$ (m, 2H), 3.35 (m, 2H), 3.24 (m, 4H), 1.70 (m, 4H), 1.53 (m, 4H), 1.39 (brs, 4H), 1.31 (m, 2H), 0.91 ppm (dd, $J=$ 6.4 and $J'=8.8$ Hz, 12H); ^{13}C NMR (75 MHz, $CDCl_3$): $\delta=175.6$, 53.4, 44.0, 38.5, 27.0, 24.8, 23.4, 21.2 ppm; IR (KBr): $\tilde{\nu}=3343$, 3292, 1631, 1550, 1524 cm^{-1}; MS (ESI): m/z: 315.5 $[M+H]^+$; elemental analysis calcd (%) for $C_{16}H_{34}N_4O_2$: C 61.11, H 10.90, N 17.82; found: C 61.32, H 11.08, N 17.74.

Compound 5a: Yield: 90%; $[\alpha]_D^{20}=-54.7$ ($c=0.025$ in $CHCl_3$); ^1H NMR (300 MHz, $CDCl_3$): $\delta=7.69$ (m, 2H), 3.33 (m, 4H), 3.17 (d, $J=3.9$ Hz, 2H), 1.88 (m, 2H), 1.31 (m, 4H), 1.10 (m, 2H) 0.88 (d, $J=7.8$ Hz, 6H), 0.82 ppm (t, $J=7.3$ Hz, 6H); ^{13}C NMR (75 MHz, $CDCl_3$): $\delta=175.1$, 59.9, 39.4, 37.9, 23.7, 16.1, 11.9 ppm; IR (KBr): 3300, 3077, 1639, 1549 cm^{-1}; MS (ESI): m/z: 287.4 $[M+H]^+$; elemental analysis calcd (%) for $C_{14}H_{30}N_4O_2$: C 58.71, H 10.56, N 19.56; found: C 58.97, H 11.05, N 19.25.

Compound 5b: Yield: 89%; $[\alpha]_D^{20}=-51.4$ ($c=0.025$ in $CHCl_3$); ^1H NMR (300 MHz, $CDCl_3$): $\delta=7.61$ (t, $J=5.6$ Hz, 2H), 3.15 (m, 6H), 1.82 (m, 2H), 1.54 (m, 2H), 1.35 (m, 6H), 0.98 (m, 2H), 0.83 (d, $J=6.8$ Hz, 6H),

0.76 (t, $J=7.3$ Hz, 6H) ppm; ^{13}C NMR (75 MHz, $CDCl_3$): $\delta=174.6$, 126.1, 59.9, 37.9, 35.5, 29.6, 23.5, 16.0, 11.7 ppm; IR (KBr): $\tilde{\nu}=3291$, 3078, 1641, 1546 cm^{-1}; MS (ESI): m/z: 301.6 $[M+H]^+$; elemental analysis calcd (%) for $C_{15}H_{32}N_4O_2$: C 59.97, H 10.74, N 18.65; found: C 60.11, H 11.16, N 18.71.

Compound 5c: Yield: 72%; $[\alpha]_D^{20}=-49.3$ ($c=0.025$ in $CHCl_3$); ^{1}H NMR (300 MHz, $CDCl_3$): $\delta=7.40$ (m, 2H), 3.17 (m, 6H), 1.87 (m, 2H), 1.45 (m, 4H), 1.29 (m, 6H), 1.00 (m, 2H), 0.85 (d, $J=6.8$ Hz, 6H), 0.79 ppm (t, $J=7.5$ Hz, 6H); ^{13}C NMR (75 MHz, $CDCl_3$): $\delta=174.1$, 126.2, 59.7, 38.4, 37.8, 27.0, 23.5, 16.1, 11.8 ppm; IR (KBr): $\tilde{\nu}=3292$, 3085, 1637, 1552 cm^{-1}; MS (ESI): m/z: 315.6 $[M+H]^+$; elemental analysis calcd (%) for $C_{16}H_{34}N_4O_2$: C 61.11, H 10.90, N 17.82; found: C 61.29, H 11.32, N 17.91.

Compound 6c: Yield: 12%; ^{1}H NMR (300 MHz, $CDCl_3$): $\delta=7.48$ (m, 3H), 7.26 (m, 1H), 7.12 (d, $J=7.3$ Hz, 2H), 3.78 (s, 4H), 3.33 (m, 8H), 2.05 (m, 2H), 1.58 ppm (m, 4H); ^{13}C NMR (75 MHz, $CDCl_3$): $\delta=171.6$, 140.0, 128.7, 127.5, 127.2, 53.8, 52.1, 38.0, 26.8 ppm; IR (KBr): $\tilde{\nu}=3315$, 1667, 1528 cm^{-1}; MS (ESI): m/z: 305.2 $[M+H]^+$; elemental analysis calcd (%) for $C_{16}H_{24}N_4O_2$: C 63.13, H 7.95, N 18.41; found: C 63.28, H 8.21, N 18.53.

Compound 7a: Yield: 27%; $[\alpha]_D^{20}=+16.1$ ($c=0.03$ in $CHCl_3/CH_3OH$, 7:3 v/v); ^{1}H NMR (300 MHz, $CDCl_3$): $\delta=7.41$ (m, 2H), 7.37 (s, 1H), 7.25 (m, 1H), 7.09 (d, $J=7.2$ Hz, 2H), 4.05 (d, $J=13.2$ Hz, 2H), 3.59 (d, $J=13.2$ Hz, 2H), 3.19 (m, 6H), 1.79 (m, 2H), 1.35 ppm (d, $J=6.6$ Hz, 6H); ^{13}C NMR (75 MHz, $CDCl_3$): $\delta=176.0$, 140.2, 128.7, 128.6, 127.5, 59.1, 53.6, 38.9, 19.9 ppm; IR (KBr): $\tilde{\nu}=3379$, 3304, 3270, 3019, 1670, 1641, 1542, 1524 cm^{-1}; MS (ESI): m/z: 305.5 $[M+H]^+$; elemental analysis calcd (%) for $C_{16}H_{24}N_4O_2$: C 63.13, H 7.95, N 18.41; found: C 63.19, H 8.32, N 18.47.

Compound 7b: Yield: 39%; $[\alpha]_D^{20}=+20.2$ ($c=0.025$ in $CHCl_3/CH_3OH$, 7:3 v/v); ^{1}H NMR (500 MHz, $CDCl_3$): $\delta=7.55$ (m, 2H), 7.46 (s, 1H), 7.28 (m, 1H), 7.13 (d, $J=7.8$ Hz, 2H), 4.05 (d, $J=13.7$ Hz, 2H), 3.65 (d, $J=13.7$ Hz, 2H), 3.30 (m, 6H), 1.72 (m, 4H), 1.36 ppm (d, $J=6.8$ Hz, 6H); ^{13}C NMR (125 MHz, $CDCl_3$): $\delta=175.3$, 140.2, 128.7, 127.4, 126.9, 57.9, 52.2, 37.3, 28.9, 19.1 ppm; IR (KBr): $\tilde{\nu}=3317$, 3085, 1630, 1541 cm^{-1}; MS (ESI): m/z: 319.2 $[M+H]^+$, 341.2 $[M+Na]^+$; elemental analysis calcd (%) for $C_{17}H_{26}N_4O_2$: C 64.12, H 8.23, N 17.60; found: C 63.92, H 8.61, N 17.51.

Compound 7c: Yield: 38%; $[\alpha]_D^{20}=-14.6$ ($c=0.025$ in $CHCl_3/CH_3OH$, 7:3 v/v); ^{1}H NMR (300 MHz, $CDCl_3$): $\delta=7.47$ (m, 2H), 7.35 (s, 1H), 7.22 (m, 1H), 7.10 (d, $J=7.8$ Hz, 2H), 3.88 (d, $J=12.7$ Hz, 2H), 3.53 (m, 2H), 3.49 (d, $J=12.7$ Hz, 2H), 3.24 (m, 2H), 2.94 (m, 2H), 1.95 (m, 2H), 1.53 (m, 4H), 1.29 ppm (d, $J=7.3$ Hz, 6H); ^{13}C NMR (75 MHz, $CDCl_3$): $\delta=174.8$, 140.2, 128.8, 128.4, 127.0, 58.6, 52.7, 38.2, 26.9, 19.6 ppm; IR (KBr): $\tilde{\nu}=3317$, 3296, 3085, 1639, 1629, 1551 cm^{-1}; MS (ESI): m/z: 333.8 $[M+H]^+$; elemental analysis calcd (%) for $C_{18}H_{28}N_4O_2$: C 65.03, H 8.49, N 16.85; found: C 65.18, H 8.76, N 16.88.

Compound 9a: Yield: 49%; $[\alpha]_D^{20}=-2.1$ ($c=0.025$ in $CHCl_3$); ^{1}H NMR (300 MHz, $CDCl_3$): $\delta=7.23$–7.14 (m, 4H), 7.03 (m, 2H), 4.00 (d, $J=13.2$ Hz, 2H), 3.46 (d, $J=13.2$ Hz, 2H), 3.12 (m, 2H), 2.96 (m, 4H), 1.93 (m, 2H), 1.69(m, 2H), 1.53 (m, 2H), 1.33 (m, 2H), 0.89 ppm (m, 12H); ^{13}C NMR (75 MHz, $CDCl_3$): $\delta=176.2$, 140.1, 129.3, 128.5, 127.6, 62.6, 54.5, 43.3, 39.3, 25.0, 23.2, 21.7 ppm; IR (KBr): $\tilde{\nu}=3317$, 1653, 1520 cm^{-1}; MS (ESI): m/z: 195.4 $[M+2H]^{2+}$; elemental analysis calcd (%) for $C_{22}H_{36}N_4O_2$: C 68.01, H 9.34, N 14.42; found: C 68.00, H 10.57, N 14.29.

Compound 9b: Yield: 40%; $[\alpha]_D^{20}=+14.7$ ($c=0.025$ in $CHCl_3$); ^{1}H NMR (300 MHz, $CDCl_3$): $\delta=7.36$–7.27 (m, 4H), 7.13 (m, 2H), 4.04 (d, $J=13.8$ Hz, 2H), 3.51 (d, $J=13.8$ Hz, 2H), 3.29 (m, 2H), 3.20 (m, 2H), 3.05 (m, 2H), 1.68 (m, 6H), 1.41 (m, 2H), 0.96 ppm (d, $J=6.1$ Hz, 12H); ^{13}C NMR (75 MHz, $CDCl_3$): $\delta=175.3$, 140.5, 128.8, 128.0, 127.0, 61.9, 53.1, 42.9, 35.9, 28.7, 25.2, 23.2, 21.9 ppm; IR (KBr): $\tilde{\nu}=3317$, 3085, 1630, 1544 cm^{-1}; MS (ESI): m/z: 202.4 $[M+2H]^{2+}$; elemental analysis calcd (%) for $C_{23}H_{38}N_4O_2$: C 68.62, H 9.51, N 13.92; found: C 68.68, H 10.22, N 13.60.

Compound 9c: Yield: 27%; $[\alpha]_D^{20}=-58.9$ ($c=0.025$ in $CHCl_3$); ^{1}H NMR (300 MHz, $CDCl_3$): $\delta=7.46$ (m, 2H), 7.41 (s, 1H), 7.30 (m, 1H), 7.18 (m, 2H), 3.90 (d, $J=12.7$ Hz, 2H), 3.64 (m, 2H), 3.55 (d, $J=12.7$ Hz, 2H), 3.24 (m, 2H), 2.98 (m, 2H), 1.78–1.58 (m, 8H), 1.39 (m, 2H), 0.97 ppm (dd, $J=2.4$ and $J'=6.4$ Hz, 12H); ^{13}C NMR (75 MHz, $CDCl_3$): $\delta=174.8$, 140.3, 128.8, 127.0, 61.9, 53.3, 42.9, 38.3, 26.9, 25.3, 23.2, 21.9 ppm; IR (KBr): $\tilde{\nu}=3315$, 3060, 1637, 1543 cm^{-1}; MS (ESI): m/z: 209.5 $[M+2H]^{2+}$; elemental analysis calcd (%) for $C_{24}H_{40}N_4O_2$: C 69.19, H 9.68, N 13.45; found: C 68.93, H 10.02, N 13.19.

Compound 10a: Yield: 56%; $[\alpha]_D^{20}=-23.9$ ($c=0.025$ in $CHCl_3$); ^{1}H NMR (500 MHz, $CDCl_3$): $\delta=7.39$ (m, 2H), 7.27 (m, 2H), 7.12 (m, 2H), 4.11 (d, $J=13.2$ Hz, 2H), 3.56 (d, $J=13.2$ Hz, 2H), 3.19 (m, 4H), 3.12 (d, $J=3.9$ Hz, 2H), 1.95 (m, 2H), 1.72 (m, 2H), 1.47 (m, 2H), 1.17 (m, 2H), 1.04 (d, $J=6.8$ Hz, 6H), 0.92 ppm (m, 6H); ^{13}C NMR (125 MHz, $CDCl_3$): $\delta=174.7$, 140.5, 128.9, 128.5, 127.5, 68.8, 54.9, 39.0, 38.4, 24.9, 16.2, 11.8 ppm; IR (KBr): $\tilde{\nu}=3314$, 1655, 1509 cm^{-1}; MS (ESI): m/z: 389.8 $[M+H]^+$; elemental analysis calcd (%) for $C_{22}H_{36}N_4O_2$: C 68.01, H 9.34, N 14.42; found: C 67.85, H 9.68, N 14.31.

Compound 10b: Yield: 41%; $[\alpha]_D^{20}=+27.0$ ($c=0.025$ in $CHCl_3$); ^{1}H NMR (300 MHz, $CDCl_3$): $\delta=7.46$ (m, 2H), 7.33 (s, 1H), 7.27 (m, 1H), 7.12 (d, $J=7.2$ Hz, 2H), 4.04 (d, $J=13.8$ Hz, 2H), 3.50 (d, $J=13.8$ Hz, 2H), 3.41 (m, 2H), 3.09–3.04 (m, 4H), 1.83 (m, 4H), 1.62 (m, 2H), 1.45 (m, 2H), 1.17 (m, 2H), 0.99 (m, 6H), 0.89 ppm (m, 6H); ^{13}C NMR (75 MHz, $CDCl_3$): $\delta=173.8$, 140.6, 128.8, 128.0, 127.1, 68.2, 53.8, 38.2, 35.6, 28.7, 25.0, 16.1, 11.9 ppm; IR (KBr): $\tilde{\nu}=3330$, 3072, 1637, 1542 cm^{-1}; MS (ESI): m/z: 202.5 $[M+2H]^{2+}$; elemental analysis calcd (%) for $C_{23}H_{38}N_4O_2$: C 68.62, H 9.51, N 13.92; found: C 68.71, H 9.73, N 14.08.

Compound 10c: Yield: 58%; $[\alpha]_D^{20}=-58.4$ ($c=0.025$ in $CHCl_3$); ^{1}H NMR (300 MHz, $CDCl_3$): $\delta=7.50$ (m, 2H), 7.41 (s, 1H), 7.30 (m, 1H), 7.16 (d, $J=6.8$ Hz, 2H), 3.89 (d, $J=12.7$ Hz, 2H), 3.64 (m, 2H), 3.55 (d, $J=12.7$ Hz, 2H), 3.12 (d, $J=4.4$ Hz, 2H), 2.99 (m, 2H), 1.88 (m, 2H), 1.65 (m, 6H), 1.46 (m, 2H), 1.14 (m, 2H), 0.99 (d, $J=6.84$ Hz, 6H), 0.90 ppm (m, 6H); ^{13}C NMR (75 MHz, $CDCl_3$): $\delta=173.4$, 140.3, 128.72, 128.67, 126.9, 68.1, 53.9, 38.04, 38.00, 26.8, 24.8, 16.1, 11.8 ppm; IR (KBr): $\tilde{\nu}=3306$, 3058, 1637, 1542 cm^{-1}; MS (ESI): m/z: 209.5 $[M+2H]^{2+}$; elemental analysis calcd (%) for $C_{24}H_{40}N_4O_2$: C 69.19, H 9.68, N 13.45; found: C 69.36, H 10.30, N 13.44.

Compound 13b: Yield: 65%; $[\alpha]_D^{20}=+89.8$ ($c=0.006$ in CH_2Cl_2); ^{1}H NMR (300 MHz, CD_3OD): $\delta=8.26$ (dd, $J=3.3$ and $J'=6.1$ Hz, 2H), 7.56 (dd, $J=3.3$ and $J'=6.1$ Hz, 2H), 7.39 (s, 2H), 4.62 (d, $J=14.8$ Hz, 2H), 3.92 (d, $J=14.3$ Hz, 2H), 2.96 (d, $J=6.1$ Hz, 2H), 2.58 (m, 2H), 2.33 (m, 2H), 2.03 (m, 2H), 0.99 (d, $J=7.2$ Hz, 6H), 0.95 (d, $J=6.6$ Hz, 6H), 0.60 ppm (m, 2H); ^{13}C NMR (75 MHz, CD_3OD): $\delta=176.9$, 137.2, 133.5, 127.1, 127.0, 125.4, 71.1, 37.8, 32.6, 28.9, 19.8, 18.5 ppm; IR (NaCl): $\tilde{\nu}=3322$, 3075, 1651, 1520 cm^{-1}; MS (ESI): m/z: 425.3 $[M+H]^+$, 447.3 $[M+Na]^+$; elemental analysis calcd (%) for $C_{25}H_{36}N_4O_2$: C 70.72, H 8.55, N 13.20; found: C 70.86, H 8.71, N 13.38.

Compound 11b: Benzyl bromide (300 µL, 2.4 mmol) was added dropwise to a refluxing mixture of compound **3b** (0.3 g, 1.1 mmol), K_2CO_3 (0.8 g, 5.7 mmol), and tetrabutyl ammonium bromide (0.05 g) in dry CH_3CN (60 mL). After being refluxed overnight, the mixture was filtered off and the solvent was evaporated under vacuum. The crude waxy solid was further purified by silica-gel column chromatography using CH_2Cl_2/CH_3OH (40:1 v/v) as eluent. Yield: 45%; $[\alpha]_D^{20}=-47.7$ ($c=0.025$ in $CHCl_3$); ^{1}H NMR (500 MHz, $CDCl_3$): $\delta=7.51$ (m, 2H), 7.32 (m, 10H), 3.79 (d, $J=13.2$ Hz, 2H), 3.64 (d, $J=12.7$ Hz, 2H), 3.28 (m, 4H), 2.96 (d, $J=4.4$ Hz, 2H), 2.11 (m, 2H), 1.64 (m, 4H), 0.96 (d, $J=6.8$ Hz, 6H), 0.90 ppm (d, $J=6.8$ Hz, 6H); ^{13}C NMR (125 MHz, $CDCl_3$): $\delta=174.0$, 139.7, 128.5, 128.2, 127.2, 68.0, 53.5, 35.6, 31.3, 30.2, 19.6, 17.9 ppm; IR (KBr): $\tilde{\nu}=3310$, 3064, 3022, 1646, 1520 cm^{-1}; MS (ESI): m/z: 453.3 $[M+H]^+$, 475.3 $[M+Na]^+$, 491.3 $[M+K]^+$; elemental analysis calcd (%) for $C_{27}H_{40}N_4O_2$: C 71.65, H 8.91, N 12.38; found: C 71.68, H 9.03, N 12.47.

CCDC-227044–227048 contain the supplementary crystallographic data for this paper. These data can be obtained free of charge via www.ccdc.cam.ac.uk/conts/retrieving.html (or from the Cambridge Crystallographic Data Centre, 12 Union Road, Cambridge CB2 1EZ, UK; fax: (+44) 1223-336-033; or e-mail: deposit@ccdc.cam.ac.uk).

Acknowledgements

The authors thank the SCIC of the University Jaume I for technical assistance with microscopy and crystallographic studies, and the Generalitat

Valenciana (Project CTDIA/2002/123) and the Spanish Ministry of Science and Technology (Project BQ2003-09215) for financial support.

[1] a) P. Terech, R. G. Weiss, *Chem. Rev.* **1997**, *97*, 3133–3159; b) D. J. Abdallah, R. G. Weiss, *Adv. Mater.* **2000**, *12*, 1237–1247; c) J. van Esch, B. L. Feringa, *Angew. Chem.* **2000**, *112*, 2351–2354; *Angew. Chem. Int. Ed.* **2000**, *39*, 2263–2266; d) O. Gronwald, E. Snip, S. Shinkai, *Curr. Opin. Colloid Interface Sci.* **2002**, *7*, 148–156.

[2] See for example: a) Y. Lin, B. Kachar, R. G. Weiss, *J. Am. Chem. Soc.* **1989**, *111*, 5542–5551; b) R. Oda, I. Huc, S. J. Candau, *Angew. Chem.* **1998**, *110*, 2835–2838; *Angew. Chem. Int. Ed.* **1998**, *37*, 2689–2691; c) G. M. Clavier, J. F. Brugger, H. Bouas-Laurent, J. -L. Pozzo, *J. Chem. Soc. Perkin Trans. 2* **1998**, 2527–2534; d) K. Yoza, N. Amanokura, Y. Ono, T. Akao, H. Shinmori, M. Takeuchi, S. Shinkai, D. N. Reinhoudt, *Chem. Eur. J.* **1999**, *5*, 2722–2729; e) N. Amanokura, Y. Kanekiyo, S. Shinkai, D. N. Reinhoudt, *J. Chem. Soc. Perkin Trans. 2* **1999**, 1995–2000; f) D. J. Abdallah, L. Lu, R. G. Weiss, *Chem. Mater.* **1999**, *11*, 2907–2911; g) R. J. H. Hafkamp, M. C. Feiters, R. J. M. Nolte, *J. Org. Chem.* **1999**, *64*, 412–426; h) J. van Esch, F. Schoonbeek, M. de Loos, H. Kooijman, A. L. Spek, R. M. Kellogg, B. L. Feringa, *Chem. Eur. J.* **1999**, *5*, 937–949; i) F. Schoonbeek, J. van Esch, R. Hulst, R. M. Kellogg, B. L. Feringa, *Chem. Eur. J.* **2000**, *6*, 2633–2643; j) M. de Loos, A. G. J. Ligtenbarg, J. van Esch, H. Kooijman, A. L. Spek, R. Hage, R. M. Kellogg, B. L. Feringa, *Eur. J. Org. Chem.* **2000**, 3675–3678; k) D. J. Abdallah, R. G. Weiss, *Langmuir* **2000**, *16*, 352–355; l) M. Kölbel, F. M. Menger, *Langmuir* **2001**, *17*, 4490–4492; m) A. Ajayaghosh, S. J. George, *J. Am. Chem. Soc.* **2001**, *123*, 5148–5149; n) U. Beginn, B. Tartsch, *Chem. Commun.* **2001**, 1924–1925; o) O. Gronwald, S. Shinkai, *Chem. Eur. J.* **2001**, *7*, 4328–4334; p) G. Wang, A. D. Hamilton, *Chem. Eur. J.* **2002**, *8*, 1954–1961; q) J. J. van Gorp, J. A. J. M. Vekemans, E. W. Meijer, *J. Am. Chem. Soc.* **2002**, *124*, 14759–14769; r) M. George, R. G. Weiss, *Langmuir* **2002**, *18*, 7124–7135; s) M. George, R. G. Weiss *Langmuir* **2003**, *19*, 1017–1025; t) C. Wang, A. Robertson, R. G. Weiss, *Langmuir* **2003**, *19*, 1036–1046; u) C. Wang, R. G. Weiss, *Chem. Commun.* **2003**, 310–311; v) G. Bühler, M. C. Feiters, R. J. M. Nolte, *Angew. Chem.* **2003**, *115*, 2599–2602; *Angew. Chem. Int. Ed.* **2003**, *42*, 2494–2497.

[3] a) N. W. Fadnavis, A. Deshpande, *Curr. Org. Chem.* **2002**, *6*, 393–410; b) I. Sato, K. Kadowaki, H. Urabe, J. H. Jung, Y. Ono, S. Shinkai, K. Soai, *Tetrahedron Lett.* **2003**, *44*, 721–724; c) J. C. Tiller, *Angew. Chem.* **2003**, *115*, 3180–3183; *Angew. Chem. Int. Ed.* **2003**, *42*, 3072–3075.

[4] a) J. H. Jung, Y. Ono, S. Shinkai, *J. Chem. Soc. Perkin Trans. 2* **1999**, 1289–1291; b) J. H. Jung, Y. Ono, S. Shinkai, *Chem. Eur. J.* **2000**, *6*, 4552–4557; c) J. H. Jung, M. Amaike, S. Shinkai, *Chem. Commun.* **2000**, 2343–2344; d) J. H. Jung, S. Shinkai, *J. Chem. Soc. Perkin Trans. 2* **2000**, 2393–2398; e) J. H. Jung, Y. Ono, S. Shinkai, *Langmuir* **2000**, *16*, 1643–1649; f) J. H. Jung, H. Kobayashi, M. Masuda, T. Shimizu, S. Shinkai, *J. Am. Chem. Soc.* **2001**, *123*, 8785–8789; g) Y. Ono, K. Nakashima, M. Sano, J. Hojo, S. Shinkai, *J. Mater. Chem.* **2001**, *11*, 2412–2419; h) J. H. Jung, S. Shinkai, *J. Incl. Phen. Macroc. Chem.* **2001**, *41*, 53–59; i) K. Sugiyasu, S. Tamaru, M. Takeuchi, D. Berthier, I. Huc, R. Oda, S. Shinkai, *Chem. Commun.* **2002**, 1212–1213; j) J. H. Jung, S. Shinkai, T. Shimizu, *Nano Lett.* **2002**, *2*, 17–20; k) J. H. Jung, H. Kobayashi, K. J. C. van Bommel, S. Shinkai, T Shimizu, *Chem. Mater.* **2002**, *14*, 1445–1447; l) J. H. Jung, K. Yoshida, T. Shimizu, *Langmuir* **2002**, *18*, 8724–8727; m) S. Kobayashi, N. Hamasaki, M. Suzuki, M. Kimura, H. Shirai, K. Hanabusa, *J. Am. Chem. Soc.* **2002**, *124*, 6550–6551; n) A. M. Seddon, H. M. Patel, S. Burkett, S. Mann, *Angew. Chem.* **2002**, *114*, 3114–3117; *Angew. Chem. Int. Ed.* **2002**, *41*, 2988–2991; o) K. J. C. van Bommel, A. Friggeri, S. Shinkai, *Angew. Chem.* **2003**, *115*, 1010–1030; *Angew. Chem. Int. Ed.* **2003**, *42*, 980–999.

[5] a) E. Ostuni, P. Kamaras, R. G. Weiss, *Angew. Chem.* **1996**, *108*, 1423–1425; *Angew. Chem. Int. Ed. Engl.* **1996**, *35*, 1324–1326; b) F. M. Menger, K. L. Caran, *J. Am. Chem. Soc.* **2000**, *122*, 11679–11691; c) P. Terech, D. Pasquier, V. Bordas, C. Rossat, *Langmuir* **2000**, *16*, 4485–4494; d) D. C. Duncan, D. G. Whitten, *Langmuir* **2000**, *16*, 6445–6452; e) D. J. Abdallah, S. A. Sirchio, R. G. Weiss, *Langmuir* **2000**, *16*, 7558–7561; f) K. Sakurai, Y. Ono, J. H. Jung, S. Okamoto, S. Sakurai, S. Shinkai, *J. Chem. Soc. Perkin Trans. 2* **2001**, 108–112; g) J. -L. Pozzo, J. -P. Desvergne, G. M. Clavier, H. Bouas-Laurent, P. G. Jones, J. Perlstein, *J. Chem. Soc. Perkin Trans. 2* **2001**, 824–826.

[6] a) H. Hidaka, M. Murata, T. Onai, *J. Chem. Soc. Chem. Commun.* **1984**, 562–564; b) K. Hanabusa, K. Okui, K. Karaki, T. Koyama, H. Shirai, *J. Chem. Soc. Chem. Commun.* **1992**, 1371–1373; c) K. Hanabusa, J. Tange, Y. Taguchi, T. Koyama, H. Shirai, *J. Chem. Soc. Chem. Commun.* **1993**, 390–392; d) K. Hanabusa, Y. Naka, T. Koyama, H. Shirai, *J. Chem. Soc. Chem. Commun.* **1994**, 2683–2684; e) H. T. Stock, N. J. Turner, R. McCague, *J. Chem. Soc. Chem. Commun.* **1995**, 2063–2064; f) K. Hanabusa, K. Hiratsuka, M. Kimura, H. Shirai, *Chem. Mater.* **1999**, *11*, 649–655; g) R. Jayakumar, M. Murugesan, C. Asokan, M. A. Scibioh, *Langmuir*, **2000**, *16*, 1489–1496; h) G. Mieden-Gundert, L. Klein, M. Fischer, F. Vögtle, K. Heuzé, J. -L. Pozzo, M. Vallier, F. Fages, *Angew. Chem.* **2001**, *113*, 3266–3267; *Angew. Chem. Int. Ed.* **2001**, *40*, 3164–3166; i) X. Luo, B. Liu, Y. Liang, *Chem. Commun.* **2001**, 1556–1557; j) J. Makarevic, M. Jokic, B. Peric, V. Tomisic, B. Kojic-Prodic, M. Zinic, *Chem. Eur. J.* **2001**, *7*, 3328–3341; k) A. Carré, P. Le Grel, M. Baudy-Floc′h, *Tetrahedron Lett.* **2001**, *42*, 1887–1889; l) N. Yamada, T. Imai, E. Koyama, *Langmuir* **2001**, *17*, 961–963; m) J. Makarevic, M. Jokic, L. Frkanec, D. Katalenic, M. Zinic, *Chem. Commun.* **2002**, 2238–2239; n) L. Frkanec, M. Jokic, J. Makarevic, K. Wolsperger, M. Zinic, *J. Am. Chem. Soc.* **2002**, *124*, 9716–9717; o) I. Ihara, T. Sakurai, T. Yamada, T. Hashimoto, M. Takafuji, T. Sagawa, H. Hachisako, *Langmuir* **2002**, *18*, 7120–7123; p) S. K. Maji, D. Haldar, A. Banerjee, A. Banerjee, *Tetrahedron* **2002**, *58*, 8695–8702; q) S. Malik, S. K. Maji, A. Banerjee, A. K. Nandi, *J. Chem. Soc. Perkin Trans. 2* **2002**, 1177–1186; r) S. A. Ahmed, X. Sallenave, F. Fages, G. Mieden-Gundert, W. M. Müller, U. Müller, F. Vögtle, J. -L. Pozzo, *Langmuir* **2002**, *18*, 7096–7101; s) S. Kiyonaka, S. Shinkai, I. Hamachi, *Chem. Eur J.* **2003**, *9*, 976–983.

[7] a) S. Bhattacharya, S. N. Ghanashyam Achayra, A. R. Raju, *Chem. Commun.* **1996**, 2101–2102; b) K. Hanabusa, R. Tanaka, M. Suzuki, M. Kimura, H. Shirai, *Adv. Mater.* **1997**, *9*, 1095–1097; c) S. Bhattacharya, S. N. Ghanashyam Achayra, *Chem. Mater.* **1999**, *11*, 3121–3132.

[8] a) E. J. de Vries, R. M. Kellogg, *J. Chem. Soc. Chem. Commun.* **1993**, 238–240; b) K. Hanabusa, Y. Matsumoto, T. Miki, T. Koyama, H. Shirai, *J. Chem. Soc. Chem. Commun.* **1994**, 1401–1402; c) K. Hanabusa, Y. Matsumoto, M. Kimura, A. Kakehi, H. Shirai, *J. Colloid Interface Sci.* **2000**, *224*, 231–244.

[9] J. Becerril, M. I. Burguete, B. Escuder, S. V. Luis, J. F. Miravet, M. Querol, *Chem. Commun.* **2002**, 738–739.

[10] a) F. Adrián, M. I. Burguete, S. V. Luis, J. F. Miravet, M. Querol, *Tetrahedron Lett.* **1999**, *40*, 1039–1040; b) J. Becerril, M. I. Burguete, F. Galindo, E. García-España, S. V. Luis, J. F. Miravet, *J. Am. Chem. Soc.* **2003**, *125*, 6677–6686.

[11] Compounds **6a** and **6b** were obtained in less than 10% yield and were not isolated from the oligomeric mixture.

[12] H. M. Tan, A. Moet, A. Hiltner, E. Baer, *Macromolecules* **1983**, *16*, 28–34.

[13] MACROMODEL 7.0, AMBER*, GB/SA solvent simulation.

[14] a) F. M. Menger, Y. Yamasaki, K. K. Catlin, T. Nishimi, *Angew. Chem.* **1995**, *107*, 616–618; *Angew. Chem. Int. Ed. Engl.* **1995**, *34*, 585–586; b) P. Babu, N. M. Sangeetha, P. Vijaykumar, U. Maitra, K. Rissanen, A. R. Raju, *Chem. Eur. J.* **2003**, *9*, 1922–1932; c) J. Makarevic, M. Jokic, Z. Raza, Z. Stefanic, B. Kojic-Prodic, M. Zinic, *Chem. Eur. J.* **2003**, *9*, 5567–5580; d) S. Kiyonaka, K. Sada, I. Yoshimura, S. Shinkai, N. Kato, I. Hamachi, *Nat. Mater.* **2004**, *3*, 58–64.

[15] The same structural parameters were found when crystals of compound **8a** were grown in benzene.

[16] Positional disorder was found in the crystal structure of compound **6a** for atoms C11 and C12 (see Supporting Information). This could be explained as a consequence of the conformational mobility of the butylenic chain at room temperature. This effect has been omitted in Figure 5 for the sake of clarity.

[17] D. T. Bong, M. R. Ghadiri, *Angew. Chem.* **2001**, *113*, 2221–2224; *Angew. Chem. Int. Ed.* **2001**, *40*, 2163–2166.

[18] As the gel fibres are in a solid state they do not contribute to the solution phase ^{1}H NMR spectra. Most likely, only monomers or solution phase pre-gel aggregates are observed.

[19] It is known that steady state NOE enhancement values are sensitive to different spin relaxation mechanisms, which in turn depend on factors such as solvent, the molecular weight of the molecules, as well as the concentration and influence of neighbouring nuclei (see T. D. W. Claridge, *High Resolution NMR Techniques in Organic Chemistry*, Pergamon, **1999**). However, all these factors are expected to be almost equivalent for the experiments described below because the molecules are very closely related analogues, the protons involved in the NOE present analogous spin systems, and all the experiments were recorded using the same concentration and solvent. Therefore, a comparison of the observed NOE enhancements of the different molecules should be possible.

[20] a) F. Mohamadi, N. G. J. Richards, T. Hendrickson, W. C. Still, *J. Comput. Chem.* **1990**, *11*, 440; b) S. J. Weiner, P. A. Kollman, D. Case, U. C. Singh, G. Alagona, S. Profeta, P. Weiner, *J. Am. Chem. Soc.* **1984**, *106*, 765; c) W. C. Still, A. Tempczyk, R. C. Hawley, T. Hendrickson, J . *Am. Chem. Soc.* **1990**, *112*, 6127; d) J.-P. Ryckaert, G. Ciccotti, H. J. C. Berendsen, *J. Comput. Phys.* **1977**, *23*, 327.

[21] a) SAINT version 6.26 A Bruker Analytical X-ray Systems, Madison, WI; b) G. M. Sheldrick, SADABS empirical absorption program, V 2.03, University of Gottingen, **1996**; c) G. M. Sheldrick, SHELXTL. 5.1 ed. Bruker Analytical X-Ray Systems, Madison WI. **1997**; d) G. M. Sheldrick, SHELX-97: A program for the refinement of crystal structures; University of Göttingen, Germany, **1997**; e) MERCURY 1.1.2, CCDC, **2002**.

Received: January 13, 2004
Published online: June 24, 2004

